INORGANIC CHEMISTRY FRONTIERS

RESEARCH ARTICLE

View Article Online
View Journal | View Issue

Cite this: *Inorg. Chem. Front.*, 2026, **13**, 3441

CO_2 conversion efficiently catalyzed under ambient conditions by new self-supported and recyclable Cu_2S

Huili Wang,[a] Tiansheng Wang,[a,b] Murielle Berlande,[a] Ahmed Subrati,[c] Sergio Moya,[c] Lionel Salmon,[b] Nathalie Daro,[d] Nathalie Audebrand,[e] Jean-René Hamon,[e] Haizhu Yu,*[f] Jean-Luc Pozzo*[a] and Didier Astruc*[a]

The catalytic activation of CO_2 under mild conditions to form value-added heterocyclic products is of paramount interest. Copper sulfides are a large class of materials, many of which are found as minerals in nature. They often show remarkable physical properties, and further studies of their catalytic properties need to be conducted. The simple compound Cu_2S was designed, its synthesis was improved, and its catalytic activities in CO_2 activation are disclosed here. Synthesized Cu_2S is shown to be an efficient heterogeneous catalyst for the carboxylation of propargylamines under ambient temperature and pressure conditions and the carboxylation of terminal alkynes under one atm CO_2 at 80 °C. CO_2 is transformed into high-value-added chemicals with a wide range of substrates with excellent yields, and the catalyst is easily reused at least 5 times without significant activity reduction. The catalytic and recycling performances are significantly better for synthesized Cu_2S compared to those of its commercial analogue. In summary, Cu_2S is a new catalyst that is simple, non-toxic, self-supported, recyclable, and practical. These findings open a general route to the catalytic properties of Cu_2S toward, not only mild CO_2 activation applications, but also a variety of other useful reactions.

Received 19th December 2025,
Accepted 9th January 2026

DOI: 10.1039/d5qi02546j

rsc.li/frontiers-inorganic

Introduction

Cu_2S, as an important semiconductor material, has shown properties and application potential in photocatalysis and electrocatalysis in recent years.[1–3] Cu_2S is a narrow bandgap semiconductor[4–6] with high conductivity involving fast electron transfer, and it performs well in electrocatalytic reduction and oxidation reactions.[7–9] The abundant active sites on the surface of Cu_2S (such as Cu^+, S^{2-}, *etc.*) help with adsorbing reactant molecules and reducing activation energy, thereby improving catalytic efficiency.[10–12] In this work, Cu_2S is used to catalyze the carboxylation of propargylamines and terminal alkynes with CO_2. Fixation of propargylamines and terminal alkynes with CO_2 produces oxazolidinone derivatives and propiolic acids, respectively, which are fine chemicals for the pharmaceuticals industry.[13]

Most of the known catalysts for carboxylation reactions are based on noble metals,[14,15] but, in order to achieve widespread application, the use of such expensive and rare noble metals should as much as possible be avoided.[16–18] In recent years, researchers have explored the application of various catalysts with propargylamines and in other carboxylation reactions.[19–23] For example, Qiao[24] developed a Cu_6–NH_2 nanocluster with a distorted octahedral Cu_6 core and NH_2-functionalized ligands, which catalyzes the cyclization of propargylamines with CO_2 under mild conditions. Cu_6–NH_2 exhibits good catalytic activity, due to its accessible active sites. The nanocluster also exhibits excellent stability, good recrystallization, and reusability, with no significant decrease in catalytic performance over five catalytic cycles. However, there are problems such as complex synthesis process and possible reaction of NH_2 sites with impurities. Kong[25] developed a long-term stable copper catalyst coordinated with sugar acetate (acetylglucose) and 2-methylimidazoline. This catalyst has multiple active sites, enabling it to efficiently capture and simultaneously activate CO_2 and propargylamines. Its turnover fre-

[a]*Université de Bordeaux, ISM, UMR CNRS No. 5255, 33405 Talence Cedex, France*
[b]*Université de Toulouse, LCC, UPR CNRS No. 8241, 31077 Toulouse Cedex, France*
[c]*Soft Matter Nanotechnology Lab, CIC biomaGUNE, Paseo Miramón, 182, 20014 Donostia-San Sebastián, Gipuzkoa, Spain*
[d]*Université de Bordeaux, CNRS, Bordeaux INP, ICMCB, UMR No 5026, 33600 Pessac, France*
[e]*Univ Rennes, ISCR (Institut des Sciences Chimiques de Rennes), UMR 6226, F-35000 Rennes, France*
[f]*Department of Chemistry and Center for Atomic Engineering of Advanced Materials, Anhui Province Key Laboratory of Chemistry for Inorganic/Organic Hybrid Functionalized Materials, Anhui University, Hefei, Anhui, 230601 People's Republic of China*

quency is as high as 880 h^{-1}, which is about 180 times that of $CuCl_2$, and the catalytic activity of Im–Cu A did not decrease after 20 repeated reactions. However, there is a potential problem of uneven distribution of active sites.[26–28] Qiu[29] proposed an efficient and stable Cu^I-anchored porous covalent organic framework Cu^I@TpBD-COF, in which TpBD is a β-ketoamine with carbonyl and amine group (–NH_2, –NHR or –NR_2), with these two groups separated by two carbon atoms. This organic framework is used to effectively catalyze the carboxylic cyclization reaction of propargylamines with CO_2 and to synthesize various functionalized oxazolidinone derivatives under mild conditions with yields of up to 99% and a turnover frequency (TOF) of 1058 h^{-1}. In addition, when simulated flue gas was used as the CO_2 source, Cu^I@TpBD-COF also showed good catalytic activity. However, the synthesis cost of COF materials is high.[30–32] Gu[33] loaded nano-Cu_2O on a ZIF-8 support to prepare Cu_2O@ZIF-8 catalyst, which can effectively catalyze the cyclization of propargylalcohols and propargylamines with CO_2 to produce valuable α-alkylene cyclic carbonates and oxazolidinones, with turnover number (TON) values of 12.1 and 19.6, respectively, and this catalyst was recycled at least 5 times. However, Cu_2O is toxic, and its TON is low.[34–36]

Despite the performances of these Cu-based systems in the cyclization of propargylamines with CO_2, these catalysts often suffer from structural complexity, high synthesis costs, toxicity issues (*e.g.*, Cu_2O), instability under ambient conditions, and limited scalability.[37–40] To address these challenges, we have developed a Cu_2S catalyst that offers a promising alternative. Cu_2S is a low-cost, environmentally friendly, structurally stable, and easy to synthesize material under mild conditions. More importantly, it provides easily accessible active sites, exhibiting high catalytic efficiency and recyclability in the cyclization of propargylamines with CO_2 even under mild conditions. This work highlights the role of Cu_2S as a powerful and sustainable copper-based catalyst platform for green CO_2 conversion chemistry. The synthesis and their effectiveness in promoting this environmentally beneficial transformation will be discussed. By harnessing the potential of such a catalyst system, this approach represents a significant step forward in the utilization of CO_2 as a valuable chemical feedstock.

Results and discussion

The preparation procedure for Cu_2S, which is based on a reported hydrothermal method[41,42] with some improvements, is described below in the Experimental section. For the identification of the Cu_2S product, XRD analysis was performed. The resultant XRD pattern is shown in Fig. 1. The diffraction pattern aligns well with the standard card of Cu_2S (ICDD PDF# PDF 00-002-1292).[43] The characteristic peaks located at approximately 27°, 32° and 46° 2θ are consistent with the standard data. No peaks of Cu(II) impurities (such as CuO or CuS) were detected, confirming that the obtained product is pure Cu_2S. It is worth noting that the diffraction peaks are relatively broad, which is indicative of the small crystallite size and the nanostructured nature of the synthesized Cu_2S. The absence of other sharp peaks confirms the high purity of the phase.

To investigate the valence state of copper in the present catalyst, which is crucial for the rationalization and understanding of the catalytic activity,[44–48] XPS measurements were performed, and the results are shown in Fig. 2. The Cu 2p XPS of synthesized Cu_2S both before and after the catalytic carboxylation reaction, as presented in Fig. 2(a) and (b), respectively, show two spin–orbit doublets with Cu $2p_{3/2}$ components at 932.4 eV (bulk monovalent Cu) and 933.2 eV (surface monovalent Cu), which indicate that Cu in the synthesized Cu_2S exclusively exists in the form of Cu(I).[49–52] Emergence of the surface Cu(I) is ascribed to the presence of surface-confined Cu-deficient Cu_2S domains wherein Cu–S covalency is weakened. The XPS data also obtained after the catalytic carboxylation reaction show that copper remains in the Cu(I) state.

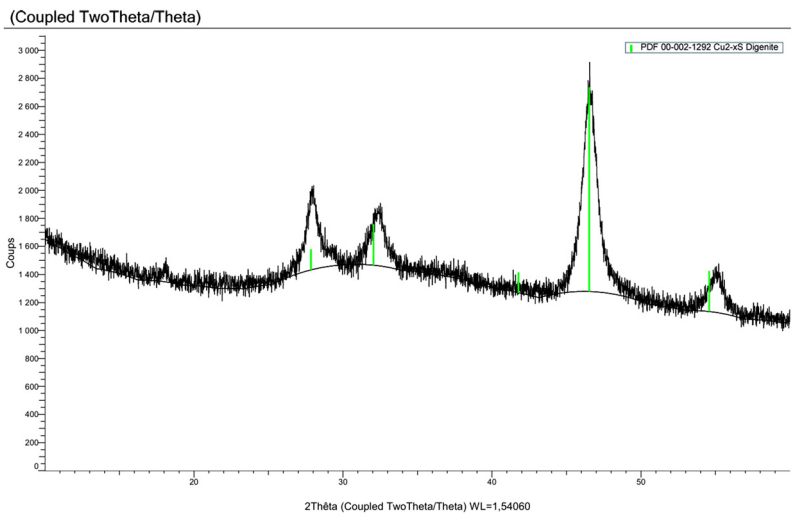

Fig. 1 XRD pattern of the synthesized Cu_2S.

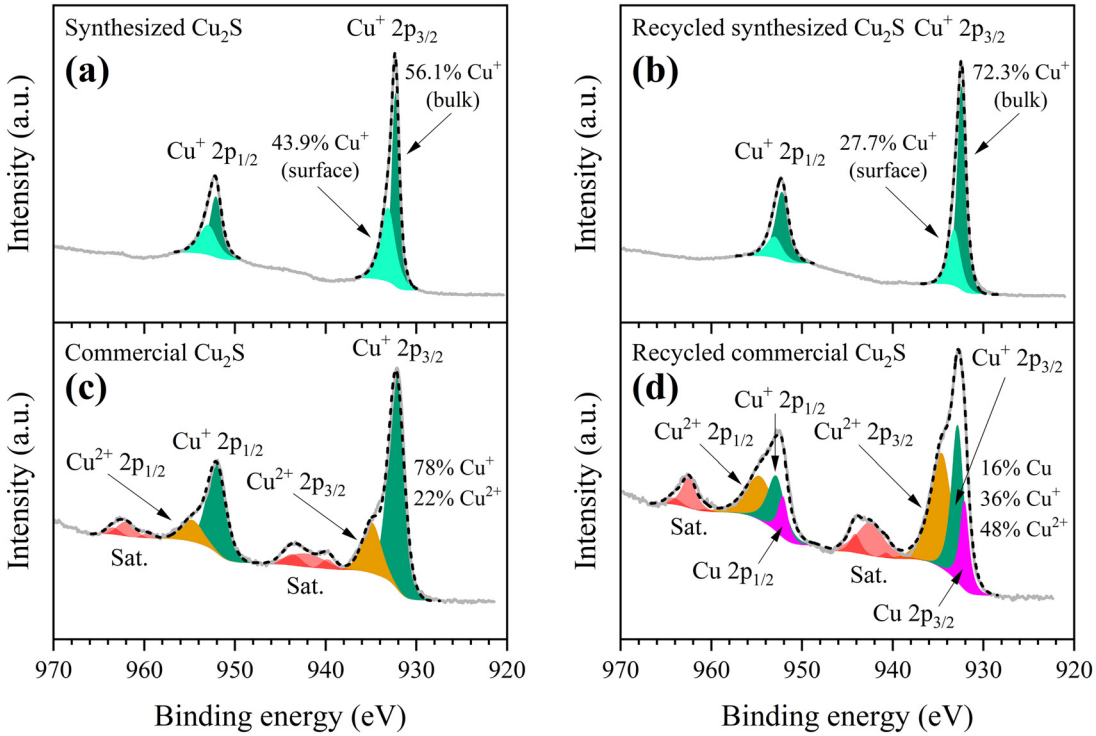

Fig. 2 High-resolution Cu 2p XPS of synthesized Cu_2S before (a) and after (b) the catalysis, and of commercial Cu_2S before (c) and after (d) catalysis. Atomic contributions of Cu, Cu^+, and Cu^{2+} to Cu 2p are reported in each panel.

However, for commercial Cu_2S (Fig. 2c and d), it was found that, in addition to the two bands around 932.5 eV and 952.4 eV for Cu(I), there were also two discernible Cu 2p spin–orbit doublets indicating the presence of Cu(0) and Cu(II) after catalysis. Therefore, the XPS results thoroughly demonstrate that the synthesized Cu_2S has a high Cu(I) purity, including after recovery from the catalytic reaction, while having a good recycling performance. The Cu XPS analysis results are summarized in Table S1.

Fig. S1(a) shows the valence band XPS of synthesized and commercially available Cu_2S before and after catalysis. Only the profiles of synthesized Cu_2S and recycled synthesized Cu_2S resemble the profile of the reference Cu_2S.[53] Fig. S1(b) shows the Auger signals for Cu, Cu LMM. Table S2 lists the Auger parameters of synthesized and commercially available Cu_2S before and after catalysis. Analysis of this parameter and inspection of peak shapes allow for assignment of copper species.[54] The synthesized Cu_2S and recycled synthesized Cu_2S respectively retained Auger parameters of 1849.93 eV and 1849.96 eV, values that are consistent with the reference Cu_2S with its Auger parameter of 1849.84 eV,[54] indicating that Cu is in the monovalent state, Cu(I), in the synthesized Cu_2S and recycled synthesized Cu_2S. However, the other entries reveal values that differ from that of Cu_2S. To demonstrate the chemical state similarities between the reference Cu_2S and synthesized Cu_2S of this work, a Cu $2p_{3/2}$ *vs.* Cu LMM Wagner (chemical state) plot is presented in Fig. S1(c). Only synthesized Cu_2S and recycled synthesized Cu_2S fall within the vicinity of the reference Cu_2S and along the diagonal line corresponding to the constant Auger parameter of 1850 eV. This confirms the sole presence of Cu(I) in synthesized Cu_2S and recycled synthesized Cu_2S. The shift of positions along the 1850 eV diagonal line can be attributed to changes in local charge density, particularly in the case of recycled synthesized Cu_2S due to presence of some nitrogen species with total atomic content of 3.15%. Another crucial difference is revealed from the analysis of the S 2p XPS, as shown in Fig. S2 and summarized in Table S3. The synthesized Cu_2S before and after catalysis retains a much larger proportion of lattice S compared to S oxide. The contrary situation is observed in the case of commercial Cu_2S before and after catalysis, where the majority of S is in the form of S oxide. Furthermore, from the S 2p XPS analysis of synthesized Cu_2S and recycled synthesized Cu_2S, we were able to probe two lattice S 2p spin–orbit doublets, corresponding to bulk and surface lattice sulfides. The bulk sulfide components have characteristically smaller full-width at half maximum (FWHM) and binding energy values when compared to the surface sulfide components. The bulk lattice sulfide exists within more crystalline domains, with higher electron delocalization, stronger Cu–S covalency, and stronger electron (back-)donation due to the higher coordination state of sulfur in the bulk as compared to the lower coordination state of sulfur in surface-bound Cu-deficient Cu_2S. It is important to note that the bulk lattice sulfide contribution increases by 10.3 atomic%, while the surface lattice sulfide contribution decreases by 7.2 atomic% after recycling

the synthesized catalyst. In addition, the Cu(I) bulk contribution increases by 16.3 atomic%, while the Cu(I) surface contribution decreases by 16.3 atomic% after recycling the synthesized catalyst. This indicates that the catalytic and recycling processes diminish the surface Cu-deficient layer bringing the catalyst closer to the stoichiometric Cu-to-S atomic ratio (Cu/S) of 2 (note the Cu/S values in Table S2). This can also serve as an explanation for the shift of recycled synthesized Cu_2S along the 1850 eV Auger parameter diagonal line shown in Fig. S1(c). The collective analysis of the Auger signal, valence band, and sulfur chemical environment, indicates that commercial Cu_2S is more susceptible to ambient oxidation and hydrolysis, both before and after catalysis, than the synthesized Cu_2S.

Fig. 3 shows the (HR-)TEM/STEM/EDS results of the synthesized Cu_2S. The sample exhibits a strong tendency to aggregate as observed in Fig. 3(a and b). Characteristic Cu_2S diffraction signals arising from distinct lattice planes were probed by HR-TEM as demonstrated in Fig. 3(c–h).[55] Cu_2S is prone to surface oxidation/contamination and this is evidenced by the presence of an ~2.3 nm amorphous layer covering crystalline grains/cores, as seen in Fig. 3(g). The STEM image shown in Fig. 3(i) reveals an aggregate of synthesized Cu_2S and EDS elemental maps of Cu and S are presented in Fig. 3(j and k). The elemental mapping shows uniform distribution of Cu and S in the sample. Values of Cu/S are seen to fluctuate between 1.9 and 2.0 averaging to 1.93 as determined from the EDS line scan, shown in Fig. 3(l). This supports the XPS findings by confirming the presence of a surface Cu-deficient Cu_2S layer.

The oxazolidinones obtained from the chemical transformation of propargylamines and CO_2 are important intermediates in the syntheses of heterocyclic compounds in organic chemistry and in the development of antibacterial drugs in medicinal chemistry.[56] Therefore, the potential application of Cu_2S in the catalytic cyclizing carboxylation of propargylamine with CO_2 was explored.[24,29] To optimize catalytic conditions, *N*-2-propyn-1-ylbenzylamine was initially selected as a model substrate (Table 1). The heterogeneous reaction with this substrate proceeded smoothly at room temperature (25 ± 1 °C) in the absence of a cocatalyst, yielding the target product, 3-benzyl-5-methylene-2-oxazolidinone, in 99% yield within 8 hours (Table 1, entry 1). Substituting TEA or cesium carbonate as the base for DBU reduced the yield to trace amounts and 50%,

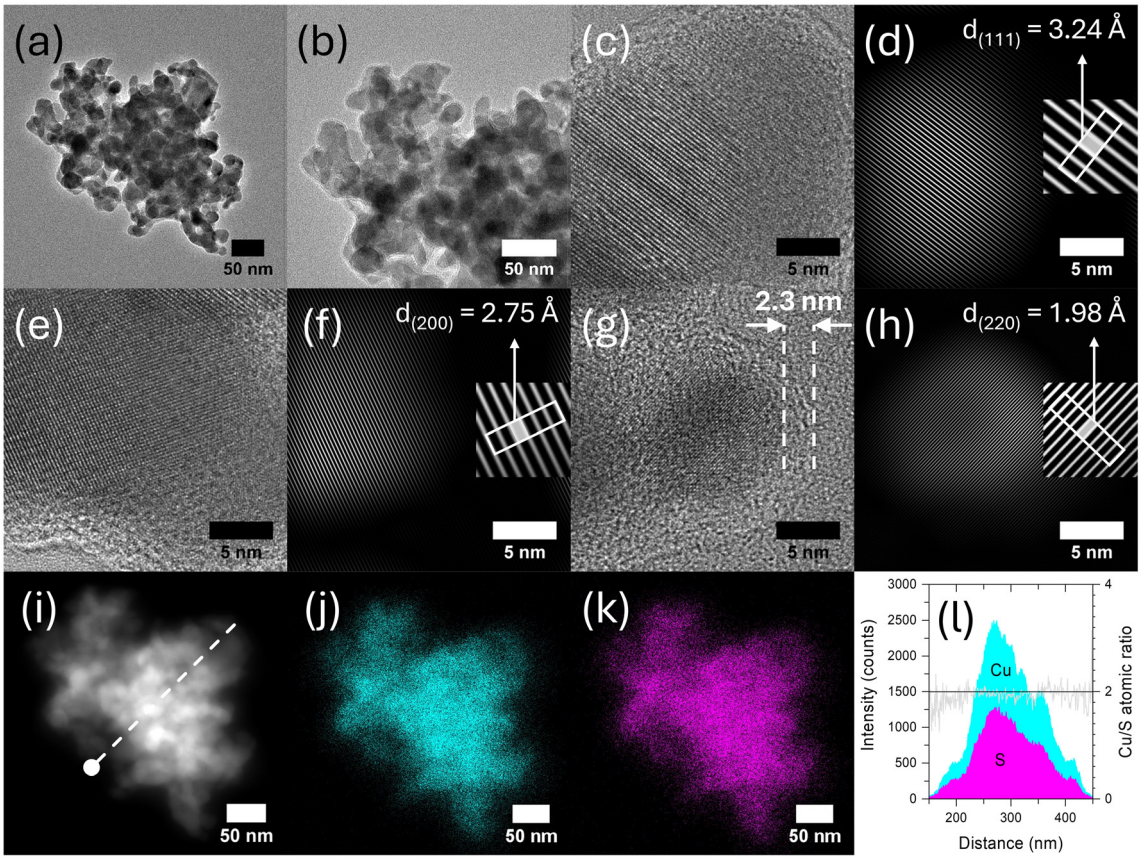

Fig. 3 (a and b) TEM images of a cluster of synthesized Cu_2S at different magnifications. (c–h) HR-TEM images revealing crystalline grains with discernible characteristic lattice planes (111), (200), and (220) with corresponding estimated lattice interplanar spacings shown as insets, obtained using fast Fourier transform (FFT) and inverse fast Fourier transform (IFFT) operations. (g) A thin amorphous layer is evident, attributed to spontaneous surface oxidation and/or contamination. (i) HAADF-STEM image of the synthesized Cu_2S cluster with corresponding EDS elemental maps for Cu (j) and S (k), and (l) an EDS line scan along the white dashed line overlaid on the HAADF-STEM image in (i), with the round head indicating the origin of the line-scan profile.

Table 1 Control experiments for carboxylation of *N*-benzylprop-2-yn-1-amine with CO_2 catalyzed by Cu_2S[a]

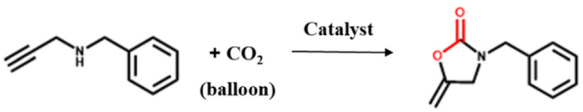

Entry	Catalyst	Substrate (mmol)	Base	Solvent	*t* (h)	Yield[b] (%)
1	Cu_2S	0.5	DBU	CH_3CN	8	99
2	Cu_2S	0.5	TEA	CH_3CN	8	Trace
3	Cu_2S	0.5	Cs_2CO_3	CH_3CN	8	50
4	Cu_2S	0.5	DBU	DMF	8	80
5	Cu_2S	0.5	DBU	CH_3OH	8	50
6	Cu_2S	0.5	DBU	DMSO	8	30
7	Cu_2S	0.5	DBU	CH_3CN	4	78
8	Cu_2S	0.1	DBU	CH_3CN	8	98
9	Cu_2S	1	DBU	CH_3CN	8	90
10	None	0.5	DBU	CH_3CN	8	0
11	Cu_2S	0.5	None	CH_3CN	8	0
12	Commercial Cu_2S	0.5	DBU	CH_3CN	8	80

[a] Reaction conditions: *N*-benzylprop-2-yn-1-amine (0.5 mmol), Cu_2S (0.005 mmol), DBU (0.5 mmol), CH_3CN (3 mL), CO_2 (balloon), room temperature. [b] The yields were determined by ^1H NMR analysis using mesitylene as the internal reference.

respectively (Table 1, entries 2 and 3). Changing the solvent from CH_3CN to DMF, CH_3OH, or DMSO reduced the yield to 80%, 50%, and 30%, respectively (Table 1, entries 4, 5, and 6). Shortening the reaction time to 4 hours reduced the yield to 78% (Table 1, entry 7). Changing the substrate dosage from 0.5 mmol to 0.1 mmol and 1 mmol, respectively, yields reached 98% and 90%, respectively (Table 1, entries 8 and 9). In the absence of catalyst or base, no target product was produced (Table 1, entries 10 and 11). Subsequently, under the same catalytic conditions, commercially available Cu_2S was used as the catalyst, achieving a product yield of 80% (Table 1, entry 12). The results demonstrate that the synthesized Cu_2S is a highly efficient catalyst for the carboxylation of propargylamine with CO_2 at room temperature and under atmospheric pressure without the need for a cocatalyst.

This study further explores the universality of the cyclization of propargylamines to yield oxazolidinone compounds.[57] Using several typical propargylamines with different substituents as raw materials, the reactions were carried out at room temperature (25 ± 1 °C) for 8 h, and the yields of the target products are shown in Table 2. These propargylamines efficiently generate the corresponding oxazolidinone compounds in high yields of at least 90% upon carboxylation reactions using CO_2 under atmospheric pressure.

To explore the recyclability of the Cu_2S catalyst, it was collected after the propargylamine transformation to oxazolidinone by reaction with CO_2 and reused under the same catalytic conditions. The data are shown in Fig. 4. On the one hand, the synthesized Cu_2S maintains its catalytic performance during the cyclization process and this only slightly decreases after five consecutive uses. On the other hand, the commercial Cu_2S catalyst shows an obvious activity decrease after five uses. This indicates that synthesized Cu_2S, unlike commercial Cu_2S, shows high stability in the catalytic reaction. To further confirm that the reaction is catalyzed by the solid Cu_2S surface rather than the leached copper species, a leaching test was performed (see Fig. 4c).[58] The reaction mixture was filtered at approximately 48% conversion to remove the solid catalyst. The filtrate was then stirred under the same reaction conditions for an additional 4 hours. We observed that the reaction proceeded negligibly after the removal of the solid catalyst. This result strongly supports the heterogeneous nature of the catalytic system.

To investigate the solubility of copper species under stoichiometric conditions, a mechanistic experiment was conducted using 0.3 mmol of substrates and 0.3 mmol of Cu_2S (1 : 1 ratio). After the reaction, the supernatant was separated and concentrated to dryness without work-up to ensure full retention of all organic and inorganic components. ICP-MS analysis data, as shown in Table 3, revealed a total leached copper mass of 2.15 mg. Relative to the total copper input (38.13 mg), this corresponds to a leaching percentage of 5.6%. This result indicates that even when the catalyst is used in stoichiometric amounts relative to the substrate, the dissolution of active copper species remains suppressed (<6%).

Table 4 presents a comparative analysis of the catalytic efficiency of the developed system in the carboxylation reaction relative to previously reported catalytic systems. Notably, the preparation of the Cu_2S catalyst does not rely on expensive or sensitive organic ligands, resulting in a simpler, lower-cost process, minimized waste generation, and reduced energy consumption, further aligning with the concept of green chemistry. This catalytic system achieves efficient conversion under mild conditions while maintaining high yields. Unlike conventional methods with poor catalyst recyclability, the Cu_2S catalyst synthesized here can be easily recovered and reused at least five times, making it more suitable for large-scale or industrial applications.

Based on the above results and previous reports, a possible mechanism for the carboxylic cyclization of CO_2 with propargy-

Table 2 Substrate scope for the carboxylic cyclization of propargylic amines with CO_2 catalyzed by Cu_2S[a]

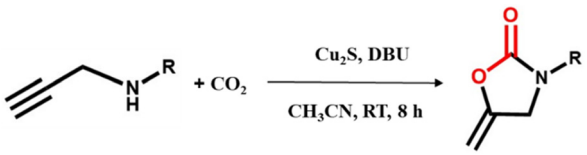

Substrate	Product	Yield[b] (%)	TON	TOF/h^{-1}
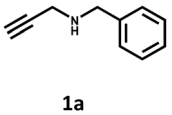 1a	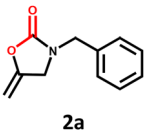 2a	99%	99	12.4
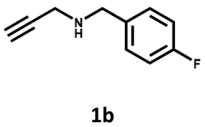 1b	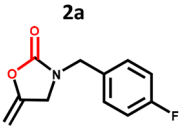 2b	97%	97	12.1
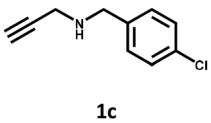 1c	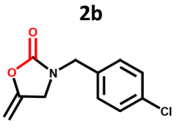 2c	94%	94	11.8
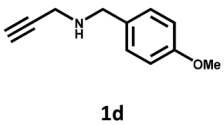 1d	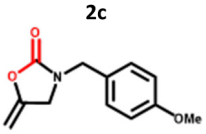 2d	98%	98	12.3
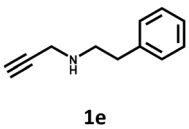 1e	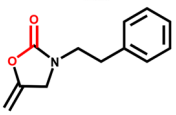 2e	97%	97	12.1
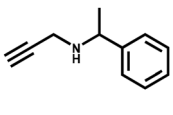 1f	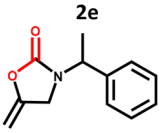 2f	93%	93	11.6
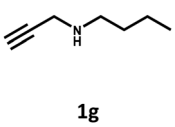 1g	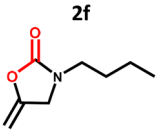 2g	95%	95	11.9
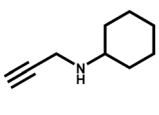 1h	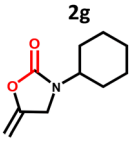 2h	94%	94	11.8
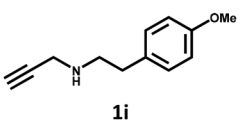 1i	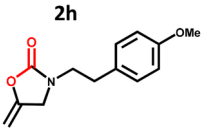 2i	93%	93	11.6
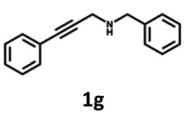 1g	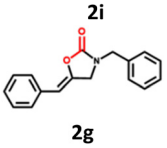 2g	96%	96	12.0

[a] Reaction conditions: 1 mmol substrate, 0.01 mmol catalyst, 1 atm CO_2 balloon, 1 mmol DBU and 3 mL CH_3CN. [b] Yields were determined by ^1H NMR with mesitylene as the internal standard.

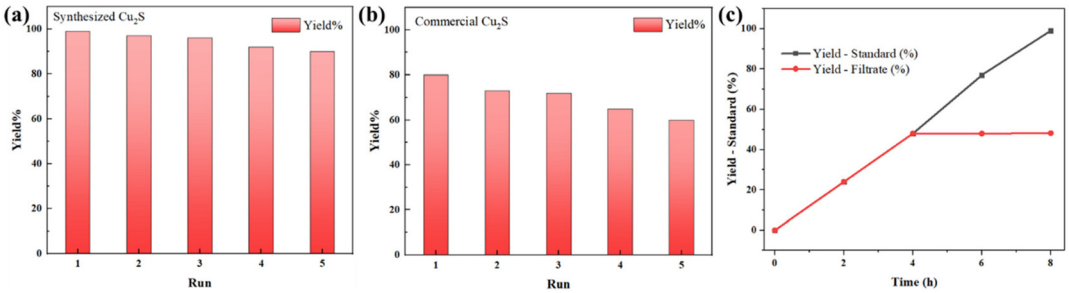

Fig. 4 Recycling performance of synthesized Cu_2S (a) and commercial Cu_2S (b) in the cyclization reaction of *N*-2-propyn-1-ylbenzenemethanamine with CO_2. (c) Leaching test.

Table 3 ICP-MS analysis of copper leaching in a stoichiometric mechanistic study[a]

Sample	Mass of residue (mg)	Total Cu detected[a] (mg)	Cu content (wt%)	Total Cu input (mg)	Leaching percentage (%)
D1	34.95	1.11	3.17	—	—
D2	23.41	0.75	3.18	—	—
D3	9.18	0.29	3.12	—	—
Total	67.54	2.15	3.18 (avg.)	38.13[b]	5.64

[a] Reaction conditions: propargylamine (0.3 mmol), DBU (0.3 mmol), Cu_2S (0.3 mmol), CH_3CN. [b] Theoretical mass of copper in 0.3 mmol Cu_2S.

Table 4 Comparison of this catalytic system with previously reported methods[29,59–61]

Entry	Catalyst	Base	CO_2 pressure (MPa)	Solvent	Temperature (°C)	Time (h)	Yield (%)	Ref.
1	Cd-Bpy-COF	DBU	Balloon	CH_3CN	60	12	99.9	53
2	Cu_2O@MOF	DBU	1.0	CH_3CN	70	12	94	26
3	Ag@2,6-FPP-TAPT	DBU	Balloon	CH_3CN	50	2	99	54
4	Ag@Pybpy-COF	Cs_2CO_3	1.0	DMF	50	0.5	99	55
5	Cu_2S	DBU	Balloon	CH_3CN	RT	8	99	This work

lamine is proposed (Fig. 5).[62–66] First, the amine reacts with CO_2 with concomitant deprotonation by DBU forming the $DBUH^+$ salt of the carbamate, which coordinates Cu through the N atom, generating intermediate **A**. Then, an oxygen atom of the carboxylic acid group coordinates to Cu, which shifts from N-coordination to π-alkyne coordination and activation in intermediate **B**. This is followed by a π to σ shift of the Cu atom, leading to isomerization to the Cu-alkenyl heterocycle **C**. Finally, protonation of **C** by $DBUH^+$ provides the metal-free target heterocyclic product, while regenerating the Cu(I) catalyst and DBU.

In recent years, the carboxylation of simple alkynes with CO_2 catalyzed by inorganic catalysts to form propiolic acid derivatives has attracted extensive attention.[67,68] For example, Yu's group[69–72] has been focusing on the application of CO_2 in organic synthesis. In addition to copper catalysis, these authors also used visible light photoredox catalysis to achieve efficient carboxylation cyclization to prepare propiolic acid compounds. Propiolic acid is not only a basic building block in medicinal chemistry but also a major component of bioactive compounds and conductive polymers.[73]

Herein, exploring the potential application of Cu_2S in the green catalytic carboxylation of terminal alkynes with CO_2 is

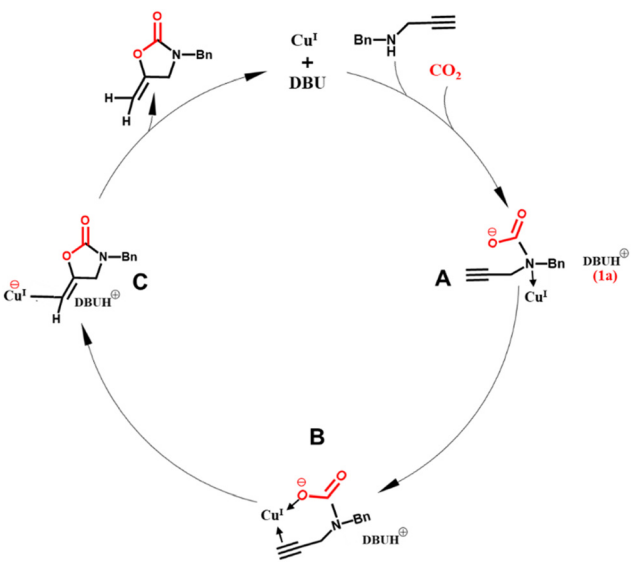

Fig. 5 Proposed reaction mechanism for the carboxylative cyclization of *N*-benzylprop-2-yn-1-amine catalyzed by synthesized Cu_2S.

Table 5 Control experiments for the carboxylation of phenylacetylene with CO_2 catalyzed by Cu_2S[a]

Entry	Catalyst	Substrate (mmol)	Base	Solvent	t (h)	T (°C)	Yield[b] (%)
1	Cu_2S	0.5	Cs_2CO_3	DMF	6	80	82
2	Cu_2S	0.5	TEA	DMF	6	80	Trace
3	Cu_2S	0.5	DBU	DMF	6	80	Trace
4	Cu_2S	0.5	Cs_2CO_3	CH_3CN	6	80	Trace
5	Cu_2S	0.5	Cs_2CO_3	DMSO	6	80	51
6	Cu_2S	0.5	Cs_2CO_3	DMF	3	80	50
7	Cu_2S	0.5	Cs_2CO_3	DMF	6	25	Trace
8	$Cu_2S/GaBr_3$	0.5	Cs_2CO_3	DMF	6	80	99
9	$Cu_2S/GaBr_3$	0.1	Cs_2CO_3	DMF	6	80	99
10	$Cu_2S/GaBr_3$	1	Cs_2CO_3	DMF	6	80	92
11	None	0.5	Cs_2CO_3	DMF	6	80	Trace
12	$Cu_2S/GaBr_3$	0.5	None	DMF	6	80	Trace
13	Commercial $Cu_2S/GaBr_3$	0.5	Cs_2CO_3	DMF	6	80	81

[a] Reaction conditions: phenylacetylene (0.5 mmol), Cu_2S (0.005 mmol), $GaBr_3$ (0.005 mmol), Cs_2CO_3 (0.75 mmol), DMF (3 mL), CO_2 (balloon). [b] Isolated yield.

also considered.[74–76] To optimize the catalytic conditions, phenylacetylene is selected as a model substrate (Table 5). The heterogeneous reaction proceeded smoothly at 80 °C, yielding the target product, phenylpropiolic acid, in 82% yield within 6 hours (Table 5, entry 1). Substituting TEA or DBU for cesium carbonate reduced the yield to trace amounts (Table 5, entries 2 and 3). Changing the solvent from DMF to CH_3CN or DMSO reduced the yield to trace amounts and 51%, respectively (Table 5, entries 4 and 5). Shortening the reaction time to 3 hours reduced the yield to 50% (Table 5, entry 6). After 6 hours of reaction at room temperature, trace amounts of the target product, phenylpropiolic acid, were afforded (Table 5, entry 7). Lewis acids are known to promote the carboxylation of alkynes by binding to one or both oxygen atoms of CO_2, further promoting C–C bond formation with CO_2 (see SI, Fig. S3). Adding the Lewis acid cocatalyst $GaBr_3$ under the conditions of entry 1 further improved the yield to 99% (Table 5, entry 8). Changing the substrate dosage from 0.5 mmol to 0.1 mmol and 1 mmol resulted in yields of 99% and 92%, respectively (Table 5, entries 9 and 10). In the absence of catalyst or base, only trace amounts of the desired product were produced (Table 5, entries 11 and 12). Subsequently, under the same catalytic conditions as entry 8 (including the presence of $GaBr_3$), commercially available Cu_2S catalyzed the reaction, yielding only 81% of the product (Table 5, entry 13). These results indicate that the synthesized Cu_2S is an efficient catalyst (more efficient than commercial Cu_2S) and achieves the green conversion of phenylacetylene with CO_2. The efficiency of the reaction, which is already very good in the absence of Lewis acid co-catalyst, is even increased under the action of the co-catalyst $GaBr_3$.

The carboxylation of terminal alkynes toward the synthesis of propiolic acid derivatives was further explored. Several typical terminal alkynes with different substituents were used as raw materials and reacted at 80 °C for 6 h. The yields of the target products are shown in Table 6. Most yields are higher than 90%. This result indicates that most terminal alkynes efficiently generate the corresponding propiolic acid derivatives and in high yield under these conditions.

Based on the above results and some previous reports,[69,72,75,76] a possible mechanism of action of the Cu_2S catalyst is proposed (Fig. S3). First, the terminal alkyne coordinates with Cu(I), and Cs_2CO_3 deprotonates the terminal alkyne to generate Cu(I) acetylide intermediate **B**. At the same time, CO_2 inserts into the carbon–copper bond, while Ga(III) coordinates with the oxygen atom to generate copper propiolate intermediate **C**. The copper propiolate intermediate **C** then reacts with free Cs ions to release cesium propiolate. At the end of the reaction, cesium propiolate is acidified to obtain the propiolic product.

Experimental

General data

Propargyl bromide, the amines, terminal alkynes, 2,3,4,6,7,8,9,10-octahydropyrimido[1,2-*a*]azepine (DBU) and commercial Cu_2S were purchased from BLD Pharm. 3-Mercaptopropionic acid (MPA) and $CuSO_4{\cdot}5H_2O$ were purchased from Thermo Scientific. H_2O_2, HNO_3 and HCl were purchased from Fisher Chemical. $GaBr_3$ was purchased from abcr GmbH. All commercial chemicals were used without further purification.

^1H NMR and ^{13}C spectra were recorded at 25 °C using a Bruker AC 300 MHz instrument. All chemical shifts are reported in parts per million (δ, ppm) and calibrated using residual protons in deuterated solvents ($CDCl_3$ at 7.26 ppm for ^1H NMR and 77.16 ppm for ^{13}C NMR; CD_3OD at 3.31 ppm for ^1H NMR and 49.00 ppm for ^{13}C NMR). The contents of carbon, hydrogen, oxygen, nitrogen, and sulfur were determined using a FlashSmart™ Elemental Analyzer (Thermo Scientific™).

The powder X-ray diffraction data were collected at room temperature on a PANalytical X'Pert MPD diffractometer (45

Table 6 Substrate scope for the carboxylic cyclization of terminal alkynes with CO_2 catalyzed by Cu_2S[a]

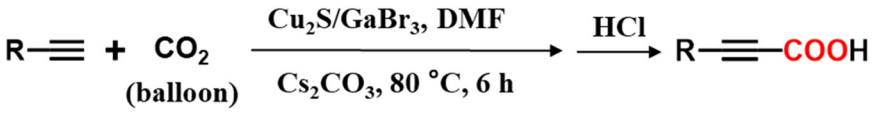

Substrate	Product	Yield[b] (%)	TON	TOF/h^{-1}
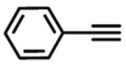 3a	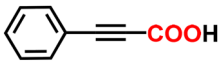 4a	99%	99	16.5
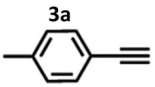 3b	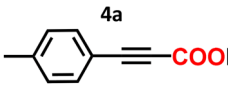 4b	91%	91	15.2
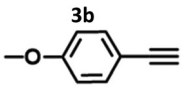 3c	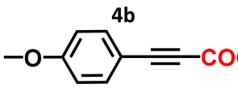 4c	90%	90	15.0
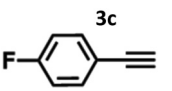 3d	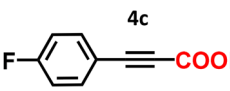 4d	91%	91	15.2
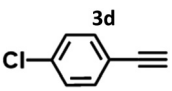 3e	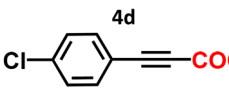 4e	88%	88	14.7
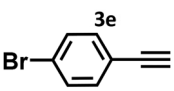 3f	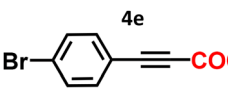 4f	89%	89	14.8
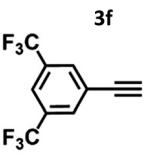 3g	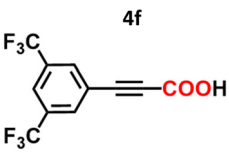 4g	88%	87	14.7
3h	 4h	97%	97	16.2
 3i	 4i	94%	94	15.7

[a] Reaction conditions: 1 mmol substrate, 0.01 mmol Cu_2S, $GaBr_3$ (0.005 mmol), 1 atm CO_2 balloon, 1.5 mmol Cs_2CO_3 and 3 mL DMF. [b] Isolated yield.

kV, 40 mA) equipped with a fast PIXcel 1D detector with Cu $K\alpha_{1,2}$ radiation in the range 6° < 2θ < 60° 2θ, a step size of 0.013° 2θ and a counting time of 38 s per step. Powdered samples were spread on a glass sampling holder. The data have been compared with the PDF5+ database from ICDD.

The supernatant after the catalytic reaction is dried under vacuum to remove the solvent. The sample was divided into three aliquots of varying masses. Each portion was weighed into a clean, sterile 15 mL polypropylene centrifuge tube (Fisherbrand™ Easy Reader™). Reagents were added sequentially to each tube under a fume hood: 375 µL of H_2O_2, 525 µL of HNO_3, and 100 µL of HCl (total volume: 1.0 mL). Upon addition of HNO_3, the solution became clear, and a tawny (HEX #C68346) precipitate was observed, indicating the presence of copper. This precipitate disappeared upon the addition of HCl. The digestion process lasted over 96 hours. At this point, all samples were completely digested, and the solutions were clear with no visible precipitate. The final digests were analyzed using a iCAP-Q ICP-MS equipment (Thermo Scientific, Bremen, Germany) equipped with an autosampler ASX-500 (CETAC Technologies, Omaha, USA).

XPS spectra were recorded using the PHI XPS VersaProbe III energy spectrometer equipped with a monochromatic 1486.6 eV Al-Kα radiation source. A focused X-ray source with X-ray beam size of 100 µm, power of 25 W, and e-beam energy of 15 kV was used. Charge neutralization was possible by using a complementary dual-beam charge neutralization method. The C 1s peak at 284.8 eV was used as the reference signal to calibrate all acquired spectra. A pass energy of 13 eV was used for the acquisition of all high-resolution spectra.

For the High-Resolution Transmission Electron Microscopy (HR-TEM) studies, samples were dispersed in hexane. Before drop casting on ultrathin carbon film placed on lacey carbon Au-coated grids (Ted Pella Inc., USA), dispersions were subjected to soft sonication until they became homogeneous. The grids were left to dry under ambient conditions prior to investigation. HR-TEM experiments were conducted on a JEOL JEM-2100F UHR electron microscope (200 kV) equipped with

an Energy Dispersive X-ray (EDS) detector (Oxford UltimMax) and two Scanning Transmission Electron Microscopy (STEM) detectors: Bright-Field (BF) and High-Angle Annular Dark-Field (HAADF). Flash column chromatography was performed using silica gel (300–400 mesh).

Synthesis of Cu_2S

Cu_2S was prepared by a reported hydrothermal method,[38] with some improvements. The specific steps are as follows (Fig. 6). In a three-necked flask, 1 mmol of $CuSO_4{\cdot}5H_2O$ was dissolved in 95 mL of distilled water and stirred for 15 minutes. 135 μL of mercapto-propionic acid (MPA) was added to the solution under continuous stirring. A yellow precipitate formed within minutes, signaling the creation of a Cu-MPA complex. The pH of the solution was then adjusted from 2 to 10 by adding 1 M NaOH solution. The mixture was subsequently heated to 100 °C, followed by the addition of 5 mL of 0.2 M $Na_2S_2O_3$ aqueous solution. The solution was refluxed at 100 °C for 7 h, resulting in the formation of a dark-brown precipitate. The mixture of Cu_2S and CuS is obtained by adjusting the pH to 5 with a small amount of dilute hydrochloric acid. After the reaction, the nanocrystal suspension was centrifuged, and the precipitate was washed three times with distilled water and three times with ethanol. The obtained Cu_2S/CuS mixture was dried under vacuum for 24 h. To eliminate trace CuS, 30 mg of the dried powder was dispersed in 10 mL of dry THF and reduced with 10 mg of $NaBH_4$ (excess) under an argon atmosphere. The reaction mixture was refluxed at 66 °C for 5 h. Finally, the product was washed three times with deionized water and ethanol, followed by drying under vacuum.

Typical procedure for the cyclization of the propargylic amines with CO_2

A mixture of Cu_2S and propargylic amine was added into a 10 mL Schlenk flask that was vacuumed and refilled 3 times with CO_2 (99.9% CO_2). DBU (0.2 equiv.) in 3 mL of acetonitrile was added into the tube. Then, the reaction mixture was stirred at room temperature (25 ± 1 °C) for 8 h. After reaction completion, the yield was determined by ^{1}H NMR analysis using mesitylene as an internal standard. To obtain the isolated product, the solvent was first removed by evaporation, then 20 mL of ethyl acetate was added to the mixture, and the mixture was washed three times (3 × 20 mL) with H_2O. The organic phase was extracted using brine water, dried over anhydrous Na_2SO_4, and filtered. The ethyl acetate solvent was removed under vacuum evaporation, and the crude product was further purified by column chromatography on silica gel (petroleum ether/ethyl acetate = 9 : 1 as an eluent) to afford the pure product. Finally, the pure products were characterized by ^{1}H NMR and ^{13}C NMR. In the recycling experiments, the catalyst is separated by centrifugation and washed three times with CH_3CN. Thereafter, the catalyst is dried at 60 °C overnight before its next use.

Catalysis of the carboxylation reaction of the terminal alkynes with CO_2

A mixture of Cu_2S (0.01 mmol), $GaBr_3$(0.01 mmol) and Cs_2CO_3 (1.5 mmol) was added into a 10 mL Schlenk flask that was vacuumed and refilled with the CO_2 balloon (99.9% CO_2) rapidly, and this operation was repeated twice more before leaving the flask connected to the CO_2 balloon. Finally, the terminal alkyne (1 mmol) in 3 mL DMF was injected into the tube. The reactor was transferred into an oil bath at the desired temperature (80 °C) with magnetic stirring (1400 rpm) for 6 h. It was then cooled down to room temperature, followed by removal of the CO_2 balloon. Then, deionized water (15 mL) was added to the reaction mixture that was stirred for 30 min. The solid catalyst was separated from the reaction mixture by centrifugation (8000 rpm, 5 min). The liquid phase obtained was washed with dichloromethane (3 × 10 mL) in a 125 mL separation funnel to keep the aqueous phase. Then, the aqueous phase was acidified to pH = 1 with concentrated aqueous HCl solution at 0 °C. The solution containing the

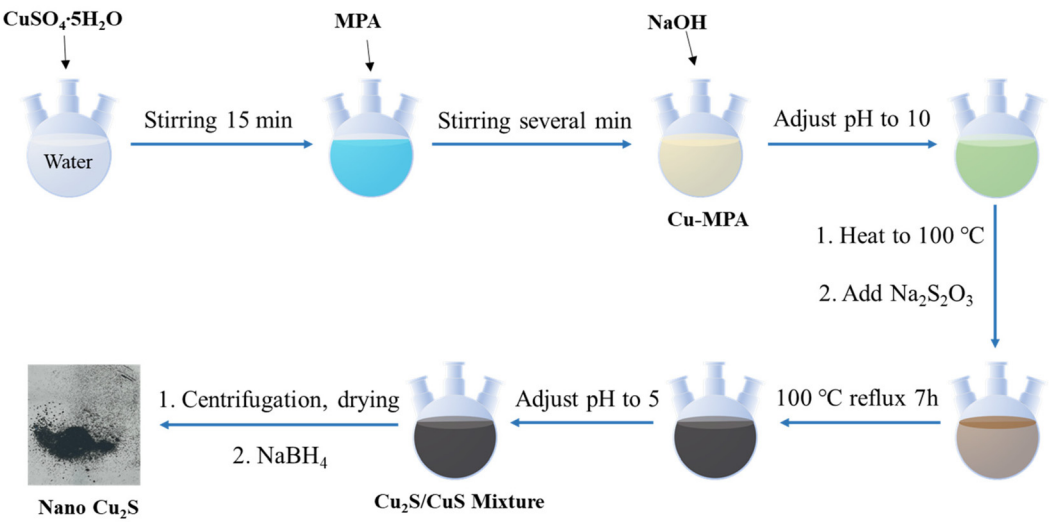

Fig. 6 Scheme of the preparation of Cu_2S.

product was then extracted with ethyl acetate. TLC was used to monitor the aqueous phase during the extraction process until no product remains. The organic phases were collected, dried over anhydrous sodium sulphate, and filtered. Then, the solvent was removed by rotary evaporation to obtain the propiolic acid. The actual mass was weighed and compared with the theoretical mass to calculate the separation yield. The final product was characterized by ^{1}H NMR. In the recycling experiments, the catalyst was separated by centrifugation and washed twice with DMF, and twice with methanol. Thereafter, the catalyst was dried at 60 °C overnight before its next use.

Conclusion

Cu_2S, a non-toxic material of high Earth abundance, which is known as an efficient p-type semiconductor for solar energy conversion,[38,39] is shown here to be a simple and efficient self-supported heterogeneous catalyst for CO_2 fixation under ambient temperature and pressure conditions in carboxylation reactions of a variety of propargylamines. In addition, it is also active for simple alkyne carboxylation under one atm CO_2. For all these CO_2 fixation reactions, the yields exceed 90% and, compared to previously reported inorganic catalysts, Cu_2S exhibits excellent stability, even in the absence of a support. It provides atom economy, one of the major rules of green chemistry, and its use therefore represents a new strategy for the resource utilization of abundant CO_2. Interestingly, the analogous compound Cu_2O is also an active catalyst for such reactions,[30] but its toxicity is well-known.[77] In conclusion, this work not only expands the application boundaries of copper-based catalysts toward C–C bond formation and heterocyclic chemistry, but also opens up a new direction for the development of green carbon capture technology.

Author contributions

H. Wang: investigation, data curation, methodology, software, validation, writing – original draft; T. Wang: contribution to the investigation; M. Berlande: contribution to the investigation and resources; A. Subrati: investigation, data curation, software, validation, writing – original draft, review and editing; S. Moya: methodology, validation, resources, funding acquisition, writing – review and editing; L. Salmon: contributions to the investigation, data curation, software; N. Daro: data curation, software; N. Audebrand: contribution to the investigation, data curation, software, validation; J.-R. Hamon, writing – review and editing; H. Yu: methodology, software, data curation, validation, resources, funding acquisition, writing – review and editing; J.-L. Pozzo: conceptualization, methodology, resources, project administration, writing – review and editing; D. Astruc: conceptualization, resources, project administration, writing – review and editing.

Conflicts of interest

The authors declare no conflict of interest.

Data availability

The data that support the findings of this study are available from the corresponding author upon reasonable request.

Supplementary information (SI): general procedure for the synthesis of propargylic amines; Table S1: Analysis summary of the high-resolution Cu 2p XPS; Fig. S1: High-resolution valence band XPS and Cu Auger signals; Table S2: Analysis summary of the Cu Auger parameter; Fig. S2: High-resolution S 2p XPS; Table S3: Analysis summary of the high-resolution S 2p XPS; Fig. S3: Proposed mechanism for the carboxylative cyclization of terminal alkyne catalyzed by Cu_2S; ^{1}H NMR and ^{13}C NMR data and spectra for the substrates and the targeted products. See DOI: **https://doi.org/10.1039/d5qi02546j**.

Acknowledgements

The financial support from the China Scholarship Council (CSC, PhD grants to H. W. and T. W.), the Centre National de la Recherche Scientifique (CNRS), the Universities of Bordeaux, Rennes and Toulouse III, and CIC biomaGUNE is gratefully acknowledged.

References

1 A. Negi, A. Chauhan and G. R. Chaudhary, *J. Cleaner Prod.*, 2024, **450**, 141829.
2 H. Liu, J. Zeng, D. Zhao, M. Yang, L. Qin, H. Chen, X. Gao, Z. Yin, R. Wang and H. Jiang, *Angew. Chem., Int. Ed.*, 2025, **64**, e202502121.
3 L. Xiang, Y. Zhang, N. Li, Y. Liu, J. Guo, B. Pang and G. Huang, *ACS Sustainable Chem. Eng.*, 2024, **12**, 14879–14889.
4 B. Zhao, X. Long, Q. Zhao, M. Shakouri, R. Feng, L. Lin, Y. Zeng, Y. Zhang, X. Fu and J. Luo, *Mater. Today Nano*, 2023, **23**, 100362.
5 S. Zhang, J. Sun and H. Ju, *Small*, 2024, **20**, 2405712.
6 Y. Zhang, H. Xu, Y. Jia, X. Yang and M. Gao, *J. Hazard. Mater.*, 2024, **472**, 134524.
7 J. Li, R. Cai, H. Mu, J. Guo, X. Zhong, J. Wang, X. Du, J. Zhang and F. Li, *ACS Catal.*, 2024, **14**, 3266–3277.
8 Y. Chang, Z. Ma, X. Lu, S. Wang, J. Bao, Y. Liu and C. Ma, *Angew. Chem., Int. Ed.*, 2023, **62**, e202310163.
9 Y. Sun, W. Sun, J. Huang, G. Li, L. Wang, S. Li, A. Meng and Z. Li, *Chem. Eng. J.*, 2023, **477**, 147016.
10 C. Q. Li and J. J. Wang, *Small*, 2024, **20**, 2404798.
11 A. Zhang, Y. Liu, J. Wu, J. Zhu, S. Cheng, Y. Wang, Y. Hao and S. Zeng, *Chem. Eng. J.*, 2023, **454**, 140317.
12 W. Sun, A. Meng, L. Wang, G. Li, J. Cui, Y. Sun and Z. Li, *J. Energy Chem.*, 2024, **94**, 29–40.
13 N. Zanda, L. Zhou, E. Alza, A. W. Kleij and M. À. Pericàs, *Green Chem.*, 2022, **24**, 4628–4633.
14 G. Kemper, M. Hölscher and W. Leitner, *Sci. Adv.*, 2023, **9**, eadf2966.

15 H. Lv, X. Wang, Y. Hao, C. Ma, S. Li, G. Li and J. Zhang, *Green Chem.*, 2023, **25**, 554–559.
16 Y. Wei, W. Zhang and J. Gao, *Green Chem.*, 2024, **26**, 5684–5707.
17 D. Raabe, *Chem. Rev.*, 2023, **123**, 2436–2608.
18 A. Zupanc, J. Install, M. Jereb and T. Repo, *Angew. Chem., Int. Ed.*, 2023, **62**, e202214453.
19 Y. Liu, T. Wang, G. M. Bousada, L. Salmon, A. Subrati, S. Moya, N. Daro, P. Hapiot, J.-L. Pozzo, H. Yu, J.-R. Hamon and D. Astruc, *Coord. Chem. Res.*, 2025, **1**, 100005.
20 W. Wang, T. Wang, S. Chen, Y. Lv, L. Salmon, B. Espuche, S. Moya, O. Morozova, Y. Yun, D. Di Silvio, N. Daro, M. Berlande, P. Hapiot, J.-L. Pozzo, H. Yu, J.-R. Hamon and D. Astruc, *Angew. Chem., Int. Ed.*, 2024, **63**, e202407430.
21 F. Chen, S. Tao, Q.-Q. Deng, D. Wei, N. Liu and B. Dai, *J. Org. Chem.*, 2020, **85**, 15197–15212.
22 Y. B. Wang, B. Y. Liu, Q. Bu, B. Dai and N. Liu, *Adv. Synth. Catal.*, 2020, **362**, 2930–2940.
23 S. Tao, Y. Wang, Q. Pan, J. Zhao, Q. Bu, F. Chen, J. Liu, B. Dai, D. Wei and N. Liu, *Green Chem.*, 2023, **25**, 6704–6716.
24 W. Qiao, Y. Wang, S. Li, R. Wang, J. Wu and S. Zang, *CCS Chem.*, 2024, **6**, 2131–2141.
25 L. Kong, Y. Liu, Z. Zhou, Z. He, Y. Bai, G. Xu, Y. Pan, H. Zhen and Y. Chen, *J. Catal.*, 2025, **443**, 115992.
26 C. Vogt and B. M. Weckhuysen, *Nat. Rev. Chem.*, 2022, **6**, 89–111.
27 S. Zhao, Y. Yang and Z. Tang, *Angew. Chem., Int. Ed.*, 2022, **61**, e202110186.
28 D. Zhou, P. Li, X. Lin, A. McKinley, Y. Kuang, W. Liu, W. Lin, X. Sun and X. Duan, *Chem. Soc. Rev.*, 2021, **50**, 8790–8817.
29 J. Qiu, X. Qi, K. Zhu, Y. Zhao, H. Wang, Z. Li, H. Wang, Y. Zhao and J. Wang, *Green Chem.*, 2024, **26**, 6172–6179.
30 Y. Zhu, L. Chen, J. Pan, S. Jiang, J. Wang, G. Zhang and K. Zhang, *Prog. Mater. Sci.*, 2024, **148**, 101373.
31 W.-T. Chung, I. M. Mekhemer, M. G. Mohamed, A. M. Elewa, A. F. El-Mahdy, H.-H. Chou, S.-W. Kuo and K. C.-W. Wu, *Coord. Chem. Rev.*, 2023, **483**, 215066.
32 M. Ma, X. Lu, Y. Guo, L. Wang and X. Liang, *TrAC, Trends Anal. Chem.*, 2022, **157**, 116741.
33 A. L. Gu, Y. X. Zhang, Z. L. Wu, H. Y. Cui, T. D. Hu and B. Zhao, *Angew. Chem., Int. Ed.*, 2022, **61**, e202114817.
34 S. Behzadinasab, M. D. Williams, J. O. Falkinham III and W. Ducker, *J. Colloid Interface Sci.*, 2023, **652**, 1867–1877.
35 W. Chen, W. Xie, Z. Gao, C. Lin, M. Tan, Y. Zhang and Z. Hou, *Adv. Sci.*, 2023, **10**, 2303694.
36 Q. Gu, J. Rong, Y. Zhang, X. Zheng, Z. Zhou, Z. Li and S. Xu, *Chem. Eng. J.*, 2025, **504**, 159143.
37 J. C. de Almeida, Y. Wang, T. A. Rodrigues, P. H. Nunes, V. R. de Mendonça, P. H. Falsetti, L. V. Savazi, T. He, A. V. Bardakova and A. V. Rudakova, *Adv. Funct. Mater.*, 2025, 2502901.
38 S. Ullah, N. Ullah, S. S. Shah, D. Guziejewski, F. Khan, I. Khan, A. Ahmad, M. Saeed, S. Khan and F. Mabood, *Renewable Sustainable Energy Rev.*, 2024, **201**, 114615.
39 S. Ali, A. Razzaq, H. Kim and S.-I. In, *Chem. Eng. J.*, 2022, **429**, 131579.
40 C. Feng, F. Raziq, H. Huang, Z. P. Wu, H. S. Aqahtani, R. Alqahtani, M. Z. Rahman, B. Chang, J. Gascon and H. Zhang, *Adv. Mater.*, 2025, **37**, 2410387.
41 Y. Zhao, H. Pan, Y. Lou, X. Qiu, J. Zhu and C. Burda, *J. Am. Chem. Soc.*, 2009, **131**, 4253–4261.
42 X. Zhang, S. Pollitt, G. Jung, W. Niu, P. Adams, J. Buhler, N. S. Grundmann, R. Erni, M. Nachtegaal, N. Ha, J. Jung, B. Shin, W. Yang and S. D. Tilley, *Chem. Mater.*, 2023, **35**, 2371–2380.
43 Y. Wang, X. Feng, Y. Xiong, S. Stoupin, R. Huang, M. Zhao, M. Xu, P. Zhang, J. Zhao and H. C. D. Abruña, *ACS Appl. Mater. Interfaces*, 2020, **12**, 17396–17405.
44 P. Basera, Y. Zhao, A. T. Garcia-Esparza, F. Babbe, N. Bothra, J. Vinson, D. Sokaras, J. Yano, S. W. Boettcher and M. Bajdich, *J. Am. Chem. Soc.*, 2025, **147**, 16070–16083.
45 S. C. Purdy, G. Collinge, J. Zhang, S. N. Borate, K. A. Unocic, Q. Wu, E. C. Wegener, A. J. Kropf, N. R. Samad and S. F. Yuk, *J. Am. Chem. Soc.*, 2024, **146**, 8280–8297.
46 M. Salehi, H. Al-Mahayni, A. Farzi, M. McKee, S. Kaviani, E. Pajootan, R. Lin, N. Kornienko and A. Seifitokaldani, *Appl. Catal., B*, 2024, **353**, 124061.
47 H. P. Sarker, A. Goswami, M. T. Tang and F. Abild-Pedersen, *ACS Catal.*, 2025, **15**, 8676–8690.
48 L. Wang, X. Yao, H. Fruehwald, D. Akhmetzyanov, M. Hanson, N. Chen, R. Smith, C. V. Singh, Z. Tan and Y. A. Wu, *Adv. Energy Mater.*, 2025, **15**, 2402636.
49 Y. Liu, R. Wang, S. Liu, Y. Xu, Z. Zhang, Y. Song and Z. Yao, *J. Colloid Interface Sci.*, 2024, **665**, 945–957.
50 Y. Luo, Z. Ruan, Z. Guo, Y. Chen, H. Lin, M. Ge and C. Zhu, *Adv. Funct. Mater.*, 2024, **34**, 2313742.
51 J. Guo, X. Wang, Z. Guo, B. Guo, Z. Wang, Z. Shang, J. Ma and M. Wu, *Carbon*, 2024, **228**, 119294.
52 G. Zhou, Y. Chen, G. Chen, H. Xu, W. Yin, B. Wang, X. Zhu, X. Ning, P. K. Chu and X. Wang, *Appl. Catal., B*, 2025, **361**, 124617.
53 B. V. Crist, *Copper Spectra, Copper(I) Sulfide - Cu_2S, International XPS Spectra-Base*, XPS Research Institute, Inc., (501c3), 2019, **https://xpsdatabase.com/copper-spectra-cu2s/**, (accessed January 23, 2026).
54 M. C. Biesinger, *Surf. Interface Anal.*, 2017, **49**, 1325–1334.
55 S. Pokhrel, J. Stahl, J. D. Groeneveld, M. Schowalter, A. Rosenauer, J. Birkenstock and L. Mädler, *Adv. Mater.*, 2023, **35**, 2211104.
56 M. Zhao, S. Huang, Q. Fu, W. Li, R. Guo, Q. Yao, F. Wang, P. Cui, C. Tung and D. Sun, *Angew. Chem., Int. Ed.*, 2020, **59**, 20031–20036.
57 X. L. Jiang, F. Y. Ren, Y. Shi, Y. Xie, S. L. Hou and B. Zhao, *CCS Chem.*, 2024, **6**, 2333–2345.
58 P. K. Giri, V. Parihar, S. Kumar and C. M. Nagaraja, *ACS Appl. Nano Mater.*, 2024, **7**, 15488–15497.
59 Y. Zhang, H. Li, X. He, A. Wang, G. Bai and X. Lan, *Green Chem.*, 2023, **25**, 5557–5565.

60 Y. Zhang, X. Lan, F. Yan, X. He, J. Wang, L. Ricardez-Sandoval, L. Chen and G. Bai, *Green Chem.*, 2022, **24**, 930–940.
61 S. Ghosh, T. S. Khan, A. Ghosh, A. H. Chowdhury, M. A. Haider, A. Khan and S. M. Islam, *ACS Sustainable Chem. Eng.*, 2020, **8**, 5495–5513.
62 X. L. Jiang, Y. E. Jiao, S. L. Hou, L. C. Geng, H. Z. Wang and B. Zhao, *Angew. Chem., Int. Ed.*, 2021, **60**, 20417–20423.
63 C. S. Cao, S. M. Xia, Z. J. Song, H. Xu, Y. Shi, L. N. He, P. Cheng and B. Zhao, *Angew. Chem., Int. Ed.*, 2020, **59**, 8586–8593.
64 Y. Zhao, J. Qiu, L. Tian, Z. Li, M. Fan and J. Wang, *ACS Sustainable Chem. Eng.*, 2016, **4**, 5553–5560.
65 X. Liu, M. Y. Wang, S. Y. Wang, Q. Wang and L. N. He, *ChemSusChem*, 2017, **10**, 1210–1216.
66 C. Du, X. Lan, G. An, Q. Li and G. Bai, *ACS Sustainable Chem. Eng.*, 2020, **8**, 7051–7058.
67 L. Xu, Y. Wang, J. Song, X. Feng, C. Wu, W. Lu, Y. Yamamoto and M. Bao, *ChemCatChem*, 2024, **16**, e202400801.
68 L. You, T. C. Han, J. R. Li, J. Guo, G. Xiong and Y. G. Sun, *J. Environ. Chem. Eng.*, 2025, **13**, 116785.
69 C. Li, X. Chen, L. Liao, Y. Gui, J. W. Yang, S. Zhang, J. Yue, X. Zhou, J. Ye, Y. Lan and Y. Dagang, *Angew. Chem., Int. Ed.*, 2025, **64**, e202413305.
70 J. Xu, J. Yue, M. Pan, Y. Chen, W. Wang, X. Zhou, W. Zhang, J. Ye and D. Yu, *Nat. Commun.*, 2025, **16**, 1850.
71 W. Wang, S. Yan, Y. Liu, J. Zhu, J.-W. Yang, J. Xu, Y. Tao, J. Li, L. Song, J. Ye and D. Yu, *J. Am. Chem. Soc.*, 2025, **147**, 23715–23723.
72 J. Ye, T. Ju, H. Huang, L. Liao and D. Yu, *Acc. Chem. Res.*, 2021, **54**, 2518–2531.
73 X. Shi, B. Sun, Q. Hu, K. Liu, P. Li and B. Liu, *Chem. Eng. J.*, 2020, **395**, 125084.
74 H. R. Li and L. N. He, *Organometallics*, 2020, **39**, 1461–1475.
75 W. J. Wang, Z. H. Sun, S. C. Chen, J. F. Qian, M. Y. He and Q. Chen, *Appl. Organomet. Chem.*, 2021, **35**, e6288.
76 T. Zhang, J. Zhong and Z. Wu, *J. Energy Chem.*, 2021, **59**, 572–580.
77 J. Zhang, Z. Zhou, B. Xiao, C. Zhou, Z. Jiang, Y. Liang, Z. Sun, J. Xiong, G. Chen and H. Zhu, *J. Environ. Manage.*, 2023, **341**, 118054.